The Journal of Chemical Physics

Electric dipole image forces in three-layer systems: The classical electrostatic model

Cite as: J. Chem. Phys. **152**, 094705 (2020); https://doi.org/10.1063/1.5142280
Submitted: 11 December 2019 . Accepted: 18 February 2020 . Published Online: 03 March 2020

Alexander M. Gabovich, Mai Suan Li, Henryk Szymczak, and Alexander I. Voitenko

The Journal of Chemical Physics ARTICLE scitation.org/journal/jcp

Electric dipole image forces in three-layer systems: The classical electrostatic model

Cite as: J. Chem. Phys. 152, 094705 (2020); doi: 10.1063/1.5142280
Submitted: 11 December 2019 • Accepted: 18 February 2020 •
Published Online: 3 March 2020

Alexander M. Gabovich,[1,a] Mai Suan Li,[2,b] Henryk Szymczak,[2,b] and Alexander I. Voitenko[1,c]

AFFILIATIONS

[1] Institute of Physics, National Academy of Sciences of Ukraine, 46 Nauky Ave., Kyiv 03028, Ukraine
[2] Institute of Physics, Polish Academy of Sciences, 32/46 Al. Lotników, Warsaw PL-02-668, Poland

[a] **Electronic mail:** gabovich@iop.kiev.ua
[b] **Electronic addresses:** masli@ifpan.edu.pl and szymh@ifpan.edu.pl
[c] **Author to whom correspondence should be addressed:** voitenko@iop.kiev.ua

ABSTRACT

General exact analytical expressions have been derived for the image force energy $W_i(Z, \varphi)$ of a point dipole in a classical three-layer system composed of dispersionless media with arbitrary constant dielectric permittivities ε_i. Here, $i = 1$–3 is the layer number, and Z and φ are the dipole coordinate and orientation angle, respectively. It was found that the long-range asymptotics $W_i(|Z| \to \infty, \varphi)$ in both covers ($i = 1, 3$) are reached unexpectedly far from the interlayer ($i = 2$). Another specific feature of the solution consists in that the interference of the fields created by polarization charges emerging at both interfaces leads to the appearance of a constant contribution inside the interlayer with a non-standard dependence on the dipole orientation angle φ. It was shown that by changing the dielectric constants of the structure components, one can realize two peculiar regimes of the $W_i(Z, \varphi)$ behavior in the covers; namely, there arises either a potential barrier preventing adsorption or a well far from the interface, both being of a totally electrostatic origin, i.e., without involving the Pauli exchange repulsion, which is taken into account in the conventional theories of physical adsorption. The results obtained provide a fresh insight into the physics of adsorption in physical electronics, chemical physics, and electrochemistry.

I. INTRODUCTION

Adsorption is a very important subject of surface science with applications to physics, chemistry, and biology.[1–17] It concerns both charged (ions) and polar or polarizable (atoms, molecules) entities, which interact electrostatically both with interfaces (system's heterogeneities)[1,5,12,14,18–25] and with one another.[10,26–29] Among those objects, there is a large class of molecules with permanent electrical dipole moments p's. Just this class of particles will be dealt with in this paper.

The interaction of a polar molecule with polarization charges induced by it at the system's interfaces leads to the appearance of an image force contribution to the total energy of the molecule. In the classical electrostatic case, when the screening ability of every medium under consideration is approximated by a corresponding dielectric constant, the image force energy for point-like dipoles near a plane interface between two adjacent semi-infinite media is described by a well-known textbook formula.[30] The latter can be easily obtained from a more "familiar" expression describing the image forces for single point charges that constitute a dipole. If one takes into account the spatial dispersion of the dielectric permittivity, i.e., if one goes beyond classical electrostatics, the results become substantially modified.[18,23,24]

Nevertheless, the results obtained in the framework of the classical approach for the constituent media still remain useful for the insight and applications. The main shortcoming of this approach consists in the appearance of an unphysical divergence of the charge potential at the interface. However, the long-range asymptotics of the obtained dependences often describe the actual behavior rather well. This circumstance was applied, e.g., in Ref. 31 (see also the references therein) when calculating far-zone asymptotics of the field induced by a point dipole located in the vacuum near the interface with a spatially inhomogeneous substrate (the two-layered system). Owing to the linearity of electrodynamic equations, the substrate is represented as a combination of homogeneous media, and the final solution is sought as a weighted superposition of well-known classical results obtained for two-layered systems. Another example concerns the problems of physical adsorption and

electrochemistry.[8–10,16] Here, the classical model is inapplicable if the potential is attractive and the resulting charge redistribution near the interface gives a crucial contribution to the studied effect. However, if the image force potential at short distances is repulsive, the indicated potential divergence only gives rise to a depletion of charges in the near-interface region and the results obtained may serve as a guide.

However, the relatively simple model of two semi-infinite spaces used so far to treat the problem of electric dipole image forces turns out insufficient to consider the behavior of a polar molecule in multilayer systems, such as semiconducting heterostructures,[32,33] adsorbates deposited above films composed of the same or different material and located on yet other substrates,[5,12–15,34–40] biological or artificial membranes,[5,25,41–49] and proteins of whatever shape.[2] The next step in this direction is the problem of calculating dipole image forces in three-layer systems.

Unfortunately, the solution of this problem has not been obtained yet, even in the framework of the classical electrostatics, not to talk about the theory taking into account the spatial dispersion of the dielectric permittivities of all layers. (An attempt to tackle the problem was made decades ago,[50] but the cited authors failed to find the solution.) On the other hand, the theory of image forces for point charges does exist.[18,23,24] Hence, in this publication, the explicit calculations have been made in the framework of the classical electrostatics. As a result, it turned out that the image force energy for a point dipole, W^{pd}, in all three layers involved can be compactly expressed in terms of known and tabulated special functions. (The generalization to a more general case making allowance for the dielectric permittivity spatial dispersion is straightforward but cumbersome.) The structure of this paper is as follows: The formulation of the problem and the working formulas are presented in Sec. II. Various possible physical consequences of those formulas are analyzed in Sec. III. Numerically obtained illustrative results are presented and discussed in Sec. IV. Conclusions can be found in Sec. V.

II. FORMULATION OF THE PROBLEM AND KEY FORMULAS

Polarization (image) forces arise between an external charge inserted into a system and polarization charges that are induced in systems with inhomogeneous distributions of dielectric permittivity. In the considered case of a three-layer ($i = 1, 2, 3$) piecewise homogeneous system composed of classical insulators with constant dielectric permittivities ε_i (see Fig. 1), polarization charges arise only at the interfaces between the layers. If two charges (1 and 2) are inserted into this system, each of them induces charges—$1'$ and $2'$, respectively—at both interfaces. Then, the image force energy for this system of two charges equals

$$W = W_{11'} + W_{22'} + W_{12'} + W_{21'}, \tag{1}$$

where $W_{ij'}$ is the interaction energy of the charge i with the polarization charge j' induced by the charge j. The first two terms in this expression describe separate image force energies for each charge, and the last two terms present the cross-interaction between each charge and the image charge of its counterpart. Note that neither the energy of direct Coulombic interaction between the charges, W_{12},

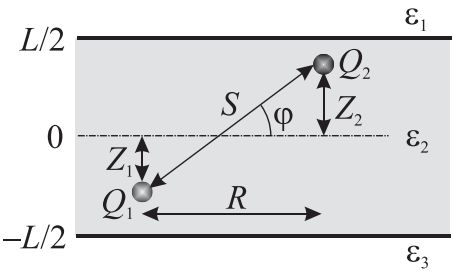

FIG. 1. A pair of interacting charges Q_1 and Q_2 located in a three-layer heterostructure with the constant dielectric permittivities of its layers $\{\varepsilon_i\} = \varepsilon_1 : \varepsilon_2 : \varepsilon_3$ at the coordinates Z_1 and Z_2, respectively, reckoned from the central plane $Z = 0$. The other parameters are as follows: S is the actual and R the lateral (along the interfaces) distance between the charges, φ is the orientation angle of the charge pair with respect to the interfaces, and L is the interlayer (medium 2) width.

nor the energy of Coulombic interaction between the induced polarization charges, $W_{1'2'}$, enters this expression, although they make a contribution to the total energy of the system.

Each summand in formula (1) can be calculated using explicit formulas obtained earlier for three-layer systems.[53,54,56,58,59] They correspond to the approximations of sharp interfaces between the layers and infinite potential barriers for specular reflection of charge carriers at those interfaces (see various versions of this approach in Refs. 52 and 60–66). In particular, it was shown that the electrostatic potential created at the point with the vertical (see Fig. 1) coordinate Z_2 in the jth layer ($j = 1, 2, 3$) by a unit point charge located at the coordinate Z_1 in the ith layer ($i = 1, 2, 3$) can be written in the form

$$\mathscr{W}_{ij}(R, Z_1, Z_2) = -2\int_0^\infty qdqD_{ij}(q, Z_1, Z_2)J_0(qR), \tag{2}$$

where $D_{ij}(q, Z_1, Z_2)$ is the electrostatic-field Green's function,[51] R is the lateral (along the interfaces) distance between the charges, and $J_0(qR)$ is the Bessel function of the first kind. The explicit forms of D_{ij} functions can be found elsewhere.[58,59] In the framework of our classical model, the potential $\mathscr{W}_{ij}(R, Z_1, Z_2)$ is the sum of the potential $\mathscr{W}_{ij}^{\mathrm{direct}}(R, Z_1, Z_2)$ created by the point unit charge itself and the potential $\mathscr{W}_{ij}^{\mathrm{im}}(R, Z_1, Z_2)$ created by the induced polarization (image) charge. Thus, the latter equals

$$\mathscr{W}_{ij}^{\mathrm{im}}(R, Z_1, Z_2) = \mathscr{W}_{ij}(R, Z_1, Z_2) - \mathscr{W}_{ij}^{\mathrm{direct}}(R, Z_1, Z_2). \tag{3}$$

The component $\mathscr{W}_{ij}^{\mathrm{direct}}(R, Z_1, Z_2)$ can be extracted from $\mathscr{W}_{ij}(R, Z_1, Z_2)$ rather easily, and the remainder $\mathscr{W}_{ij}^{\mathrm{im}}(R, Z_1, Z_2)$ is exactly the potential created at the point Z_2 by the polarization charges induced in the system by the unit charge located at the point Z_1. The relevant expressions serve as a starting point to find each term on the right-hand side of Eq. (1). However, first of all, we should reduce the number of required $\mathscr{W}_{ij}^{\mathrm{im}}$ functions ($i, j = 1, 2, 3$). In the case of a point dipole, we need only expressions for the $\mathscr{W}_{ij}^{\mathrm{im}}$ functions with $i = j$ because both the dipole charges have to be located in the same layer. Accordingly, the component $\mathscr{W}_{ii}^{\mathrm{direct}}(R, Z_1, Z_2)$ equals

$$\mathscr{W}_{ii}^{\text{direct}}(R,Z_1,Z_2) = \frac{1}{\varepsilon_i}\int_0^\infty dq J_0(qR)\exp(-q|Z_1-Z_2|) = \frac{1}{\varepsilon_i\sqrt{R^2+|Z_1-Z_2|^2}} = \frac{1}{\varepsilon_i S}, \tag{4}$$

where S is the distance between the point charge and the point at which the potential is calculated (see Fig. 1). It is natural that $\mathscr{W}_{ii}^{\text{direct}}(R,Z_1,Z_2)$ diverges at $S\to 0$ because the self-energy of point charge is infinite in classical electrostatics. However, this divergence is not detrimental at all for all subsequent calculations because exactly the same term is contained in $\mathscr{W}_{ii}(R,Z_1,Z_2)$ so that operation (3) eliminates the self-energy divergence. However, the existence of the latter is crucial to correctly calculate the interaction energy between external charges (rather than the image force energy), as has been shown by us earlier.[58,59]

Note that the indicated divergence appears only in the classical theory. If the screening by itinerant electrons or mobile ions in electrolyte solutions is taken into account, the quantity $\mathscr{W}_{ii}^{\text{direct}}(S\to 0)$ becomes finite. In metals, it represents a negative mean bulk electrostatic energy of an electron, being a finite difference between the infinite Coulomb self-energy of the unscreened charge and an infinite energy of the surrounding electron cloud.[64,67] In the more sophisticated approaches describing real solids with periodic ion lattices, it is called the "mean inner potential" and can be probed experimentally.[12,68] At the same time, the so renormalized image force energy $\mathscr{W}_{ii}^{\text{im}}(R=0,Z_1=Z_2=Z)$ in the classical electrostatic approach also has the textbook divergence $\sim Z^{-1}$ at the medium i surface.[30] The account of the spatial dispersion of the dielectric permittivity destroys this divergence as well, and the quantity $\mathscr{W}_{ii}^{\text{im}}(S=0)$ becomes finite at the interface.[53,54]

After operation (3), every $\mathscr{W}_{ii}^{\text{im}}(R,Z_1,Z_2)$ is a certain finite linear sum of integrals such as[58]

$$\int_0^\infty dq \frac{\exp(-q|Z_1\pm Z_2\pm L|)}{1-\theta\exp(-2qL)}J_0(qR), \tag{5}$$

where

$$\theta = \frac{\varepsilon_1-\varepsilon_2}{\varepsilon_1+\varepsilon_2}\times\frac{\varepsilon_2-\varepsilon_3}{\varepsilon_3+\varepsilon_2} \tag{6}$$

is the dielectric mismatch parameter and L is the width of interlayer 2.

Now, let us apply this result to two point charges Q_1 and Q_2 located in the ith layer at the coordinates Z_1 and Z_2, respectively, and at the lateral distance R from each other (Fig. 1). According to that said above, the summands on the right-hand side of Eq. (1) equal

$$\begin{aligned} W_{11'} &= Q_1Q_1\mathscr{W}_{11}^{\text{im}}(R=0,Z_1,Z_1),\\ W_{22'} &= Q_2Q_2\mathscr{W}_{22}^{\text{im}}(R=0,Z_2,Z_2),\\ W_{12'} &= Q_1Q_2\mathscr{W}_{12}^{\text{im}}(R,Z_1,Z_2),\\ W_{21'} &= Q_1Q_2\mathscr{W}_{21}^{\text{im}}(R,Z_2,Z_1), \end{aligned} \tag{7}$$

with $W_{12'}=W_{21'}$ in line with Green's reciprocity theorem. When passing to the dipole scenario, attention has to be paid that in this case the charges Q_1 and Q_2 are not arbitrary but are related as $Q_1=-Q_2=Q$. Furthermore, the polarization charges at the interfaces are also not independent but appear only as an induced response to the electric field created by the external charges. Formally, this circumstance can be taken into account by means of the gradual "Güntelberg charging process,"[69–71] when the charge is artificially changed from zero to its actual value. As a result, the calculated sum has to be divided by 2 so that the image force energy for an extended dipole located in the ith layer equals

$$W_i^{\text{ed}} = \frac{Q^2}{2}\left[W_{11'}(0,Z_1,Z_1)+W_{22'}(0,Z_2,Z_2)-2W_{12'}(R,Z_1,Z_2)\right]. \tag{8}$$

Finally, we have to make a transition to the point dipole. Let the dipole moment be equal to $P=QS$. We should change the parameters Q, R, Z_1, and Z_2 in Eq. (8) in such a way that the distance S between the charges (the dipole arm) would vanish, but the P-value would remain constant. For this purpose, let us put (see Fig. 1) $Z_1=Z_0-\frac{S}{2}\sin\varphi$, $Z_2=Z_0+\frac{S}{2}\sin\varphi$, and $R=S\cos\varphi$, where Z_0 is the coordinate of the dipole center and φ is the dipole orientation angle reckoned from the plane parallel to the interfaces. Then,

$$W_i^{\text{pd}}(Z_0) = \lim_{S\to 0}\frac{S^2}{S^2}W_i^{\text{ed}} = P^2\left[\frac{d^2W_i^{\text{ed}}}{dS^2}\right]_{S=0}. \tag{9}$$

The procedure of passing to the limit $S\to 0$ (so that $R\to 0$) is remarkable from the technical point of view because it eliminates the "detrimental" influence of the Bessel function in Eq. (5)—namely, $J_0(qR\to 0)\to 1$—and the final result can be expressed in terms of special functions, namely, the Lerch transcendent[72]

$$\Phi(\alpha,\mu,\nu) = \frac{1}{\Gamma(\nu)}\int_0^\infty \frac{x^{\nu-1}\exp(-\mu x)dx}{1-\alpha\exp(-x)} = \sum_{n=0}^\infty \frac{\alpha^n}{(\mu+n)^\nu}, \tag{10}$$

where $\Gamma(\nu)$ is the gamma function.

In the point-dipole limit, only one length scale survives; this is the interlayer width L. Therefore, it is reasonable to introduce the dimensionless quantities $z=Z/L$ and $w_i=L^3W_i^{\text{pd}}/P^2$. Then,

$$w_1\left(z>\tfrac{1}{2}\right) = \frac{\left(1+\sin^2\varphi\right)}{16(\varepsilon_2+\varepsilon_1)}\times\left\{\frac{(\varepsilon_1-\varepsilon_2)}{\varepsilon_1\left(z-\frac{1}{2}\right)^3} + \frac{4\varepsilon_2(\varepsilon_2-\varepsilon_3)\Phi\left(-\theta,\frac{1}{2}+z,3\right)}{(\varepsilon_2+\varepsilon_3)(\varepsilon_2+\varepsilon_1)}\right\}, \tag{11}$$

$$w_2\left(-\tfrac{1}{2}<z<\tfrac{1}{2}\right) = \frac{(\varepsilon_1-\varepsilon_2)(\varepsilon_3-\varepsilon_2)\left(1-3\sin^2\varphi\right)\Phi(-\theta,1,3)}{8(\varepsilon_1+\varepsilon_2)\varepsilon_2(\varepsilon_2+\varepsilon_3)} + \frac{(\varepsilon_2-\varepsilon_3)\left(1+\sin^2\varphi\right)\Phi\left(-\theta,\frac{1}{2}+z,3\right)}{16\varepsilon_2(\varepsilon_2+\varepsilon_3)} + \frac{(\varepsilon_2-\varepsilon_1)\left(1+\sin^2\varphi\right)\Phi\left(-\theta,\frac{1}{2}-z,3\right)}{16(\varepsilon_1+\varepsilon_2)\varepsilon_2}, \tag{12}$$

$$w_3\left(z<-\tfrac{1}{2}\right)=\frac{\left(1+\sin^2\varphi\right)}{16(\varepsilon_2+\varepsilon_3)}\times\left\{-\frac{(\varepsilon_3-\varepsilon_2)}{\varepsilon_3\left(z+\frac{1}{2}\right)^3}+\frac{4\varepsilon_2(\varepsilon_2-\varepsilon_1)\Phi\left(-\theta,\frac{1}{2}-z,3\right)}{(\varepsilon_1+\varepsilon_2)(\varepsilon_2+\varepsilon_3)}\right\}. \tag{13}$$

It is evident that w_1 can be transformed into w_3 and vice versa by making the substitutions $\varepsilon_1 \rightleftarrows \varepsilon_3$ and $z \rightleftarrows -z$.

Below, the terms including the dielectric permittivities of all three media will be referred to as interference ones, namely, these are the second terms in the braces in w_1 and w_3, as well as all terms in w_2.

III. ANALYSIS OF THE SOLUTION

Solutions (11)–(13) demonstrate some interesting features. Let us consider, e.g., medium 1 and its interface with medium 2. In the long-range limit $z \to \pm\infty$, we have

$$\Phi(-\theta, z\to\pm\infty, 3)\to\frac{1}{z^3(1+\theta)}$$

so that the expression for the image force energy of a dipole located in medium 1 far away from interlayer 2 looks like

$$w_1(z\to\infty)=\frac{\left(1+\sin^2\varphi\right)(\varepsilon_1-\varepsilon_3)}{16(\varepsilon_1+\varepsilon_3)\varepsilon_1}\times\frac{1}{\left(z-\frac{1}{2}\right)^3}. \tag{14}$$

This expression does not include the dielectric permittivity ε_2 of the slab. Thus, it appears that, very far away from the thin film ($Z \gg L$), the dielectric response of substrate 3 determines the interaction of the dipole with the interfaces. In other words, the influence of interlayer 2 between media 1 and 3 becomes negligible.

In the symmetric case $\varepsilon_1 = \varepsilon_3$, asymptotics (14) is not enough, and the next term in the long-range expansion of the Lerch transcendent[72] has to be taken into account. As a result, we obtain

$$w_1(z\to\infty,\varepsilon_1=\varepsilon_3)=\frac{3\left(1+\sin^2\varphi\right)\left(\varepsilon_1^2-\varepsilon_2^2\right)}{64\varepsilon_1^2\varepsilon_2}\times\frac{1}{z^4} \tag{15}$$

so that the image force energy now vanishes more rapidly at infinity than it does in the non-symmetric case.

In the short-range limit $z \to \frac{1}{2}$ achieved from the medium-1 side, the first term in the braces in Eq. (11) is singular and dominates so that

$$w_1\left(z\to\tfrac{1}{2}+0\right)\to\frac{\left(1+\sin^2\varphi\right)(\varepsilon_1-\varepsilon_2)}{16(\varepsilon_2+\varepsilon_1)\varepsilon_1}\times\frac{1}{\left(z-\frac{1}{2}\right)^3}. \tag{16}$$

Now, this asymptotics does not contain the dielectric permittivity ε_3 of the other cover (medium 3). The same situation takes place in the limit $w_2\left(z\to\frac{1}{2}-0\right)$ when we approach the $z=\frac{1}{2}$ interface from the other side, namely, from the slab one. In this limit, the first two terms on the right-hand side of formula (12) are finite, whereas the third term is singular, i.e., dominates. The limit

$$\lim_{\mu\to 0}\Phi(\alpha,\mu,\nu)\to\frac{1}{\mu^\nu}$$

[see Eq. (10)] is not sensitive to the parameter α so that

$$w_2\left(z\to\tfrac{1}{2}-0\right)\to\frac{(\varepsilon_2-\varepsilon_1)\left(1+\sin^2\varphi\right)}{16(\varepsilon_1+\varepsilon_2)\varepsilon_2}\times\frac{1}{\left(z-\frac{1}{2}\right)^3}. \tag{17}$$

Formulas (16) and (17) are the exact solutions of the problem for image forces in the case of a point dipole in a two-layer system of classical insulators. It seems rather reasonable because the interaction of the dipole in the three-layer system with polarization charges emerging at the nearest interface $\left(z=\frac{1}{2}\right)$ overcomes the interaction with more distant polarization charges emerging at the far interface $\left(z=-\frac{1}{2}\right)$.

By the way, the required formulas for the two-layer geometry can be easily reproduced from our result, e.g., by putting $\varepsilon_1 \neq \varepsilon_2 = \varepsilon_3$, i.e., by equating media 2 and 3, and thus transforming the system into that composed of two semi-spaces separated by a plane interface at $z=\frac{1}{2}$. Then, only the first term in the braces on the left-hand side of Eq. (11), the last term on the right-hand side of Eq. (12), and the last term in the braces on the left-hand side of Eq. (13) survive. Taking into account that now $\theta = 0$ [see Eq. (6)] and

$$\Phi(0,\mu,\nu)=\frac{1}{\mu^\nu}$$

[see Eq. (10)], we obtain that

$$w_1\left(z>\tfrac{1}{2}\right)=\frac{(\varepsilon_1-\varepsilon_3)\left(1+\sin^2\varphi\right)}{16(\varepsilon_3+\varepsilon_1)\varepsilon_1}\times\frac{1}{\left(z-\frac{1}{2}\right)^3}, \tag{18}$$

$$w_2\left(-\tfrac{1}{2}\le z<\tfrac{1}{2}\right)=w_3\left(z\le-\tfrac{1}{2}\right)=\frac{(\varepsilon_3-\varepsilon_1)\left(1+\sin^2\varphi\right)}{16(\varepsilon_1+\varepsilon_3)\varepsilon_3}\times\frac{1}{\left(z-\frac{1}{2}\right)^3}. \tag{19}$$

Hence, the divergence at $z=-\frac{1}{2}$ disappears, the image force energy in layers 2 and 3 is described by the common formula (19), and formulas (18) and (19) are equivalent to those well-known from classical electrostatics for a point dipole in a two-layer system with the interface at $z=\frac{1}{2}$. The limiting formulas (16) and (17) are absolutely identical to formulas (18) and (19), since $\varepsilon_2 = \varepsilon_3$ in this case. It is easy to verify that an analogous result (with an accuracy of the replacement $\varepsilon_1 \rightleftarrows \varepsilon_3$ and $\frac{1}{2}-z \rightleftarrows \frac{1}{2}+z$) is obtained if we put $\varepsilon_1 = \varepsilon_2 \neq \varepsilon_3$, but the separating interface is located at $z=-\frac{1}{2}$.

Finally, let us consider a symmetric configuration with $\varepsilon_1 = \varepsilon_3$. Then, it is easy to see that the difference $\varepsilon_1 - \varepsilon_2 (= \varepsilon_3 - \varepsilon_2)$ becomes a factor in each of expressions (11)–(13). This means that if we put $\varepsilon_1 = \varepsilon_2 = \varepsilon_3$, then, according to the indicated formulas,

$$w_1\left(z\ge\tfrac{1}{2}\right)=w_2\left(-\tfrac{1}{2}\le z\le\tfrac{1}{2}\right)=w_3\left(z\le-\tfrac{1}{2}\right)=0 \tag{20}$$

simultaneously in all layers. In other words, the image forces vanish, as it has to be in a homogeneous system. Thus, all limiting cases for configurations with reduced layer numbers are correctly reproduced.

Let us consider once more asymptotics (14) and (16) for w_1 in cover 1 if $\varepsilon_1 \neq \varepsilon_2 \neq \varepsilon_3$. Their signs are determined by the difference $\varepsilon_1 - \varepsilon_3$ in the former case and the difference $\varepsilon_1 - \varepsilon_2$ in the latter one. The positive w-sign corresponds to the repulsion of the dipole from the interface, and the negative one corresponds to the attraction to the latter. Therefore, in the case, e.g., $\varepsilon_2 < \varepsilon_1 < \varepsilon_3$, we inevitably obtain a singular repulsion of the dipole from the $z = \frac{1}{2}$ interface (here, $\varepsilon_1 > \varepsilon_2$) and a vanishing attraction at asymptotically large distances $z \to \infty$ (here, $\varepsilon_1 < \varepsilon_3$). Those two behaviors can be smoothly matched with each other only in the case of a potential well in the intermediate region $\frac{1}{2} < z < \infty$. Thus, the formation of a potential well in medium 1 is unavoidable for the indicated relationships among the dielectric permittivities of the layers. A similar consideration brings us to a conclusion that, in the case $\varepsilon_3 < \varepsilon_1 < \varepsilon_2$, there inevitably arises a potential barrier for a dipole in layer 1. Of course, the well depth and the barrier height are governed by the specific ε_i values, and they will be illustrated numerically in Sec. IV. Hence, a proper selection of heterostructure materials with specific dielectric permittivities allows adsorption or repulsion to be controlled electrostatically.

The behavior of the polarization energy in the slab (medium 2) is much more intricate, as has been recognized long ago,[73,74] although the explicit expressions for $w_2(z)$ have not been found. From Eq. (12), it is clearly seen that there are two terms, each of which corresponding to "its own" interface. The implicit influence of either interface on the term generated by polarization charges positioned at its counterpart does exist. However, it occurs far enough from the interfaces because the mismatch parameter θ depends on all dielectric constants [see Eq. (6)]. Of course, this influence disappears close to any slab boundary, when the first term in series (10) diverges. Then, the conventional behavior similar to formula (17) is recovered near the interfaces $z = \pm\frac{1}{2}$.

There is an additional interference in the interlayer between the polarization charges. It is described by the position-independent (z-independent) term, namely, the first term in Eq. (12). This term is symmetrical with respect to ε_1 and ε_3. It can be considered as an analog of the term found in the case of the point-charge image force energy in three-layer systems.[56] It is also intriguing that its angular dependence is different from the conventional one, the latter being exhibited by all other terms in Eqs. (11)–(13) and favoring the normal dipole orientation with respect to the interfaces.

The obtained general formulas have interesting consequences that will be treated in Sec. IV numerically in more detail.

IV. NUMERICAL ILLUSTRATIONS AND DISCUSSION

According to the formulas obtained in Secs. II and III, the qualitative behavior of the dependence $w(z)$ in the classical dispersionless three-layer system with the dielectric permittivities of the layers $\{\varepsilon_i\} = \varepsilon_1 : \varepsilon_2 : \varepsilon_3$ can be understood on the basis of the following simple rules: (i) For a point dipole in the medium with the dielectric permittivity ε, the medium with the dielectric permittivity $\varepsilon' > \varepsilon$ is attractive and the medium with $\varepsilon'' < \varepsilon$ is repulsive. (ii) If a dipole is located very close to any of the interfaces, it looks like only one (the nearest) medium is located on the other side from this interface. If the relevant dielectric permittivities are different, the image force energy diverges on each side of the interface with the divergence sign being determined by rule (i). If the dielectric permittivities are identical, those two media form a common unified medium (the interface disappears), so that $w(z)$ becomes a smooth function there, and the three-layer configuration degenerates into the two-layer one. (iii) A dipole located sufficiently far from the interlayer does not feel it (the semi-infinite substrate hinders the contribution of the very narrow slab).

Illustrations of the $w(z)$ behavior in all layers are displayed in Figs. 2(a)–4(a). The sets of ε_i were intentionally chosen to be non-symmetrical in order to avoid any possible occasional simplifications. Those figures represent three possible situations for the curves $w_2(z)$: the existence of a maximum (Fig. 2), an inflection point (Fig. 3), and a minimum (Fig. 4) in the interlayer. The characteristic points are not located in the slab center ($z = 0$) because of the indicated non-symmetricity of the ε_i-sets. In addition, it is easily seen that there is no qualitative difference between the behavior of $w_2(z)$ for limiting values of the orientation angle φ. The values of $w_{1,3}(z, \varphi = \pi/2)$ in the covers are twice their counterparts $w_{1,3}(z, \varphi = 0)$ [see Eqs. (11) and (13)] and are shown for completeness.

The overall panorama depicted in Figs. 2(a)–4(a) cannot reveal certain peculiar details of the $w_i(z)$ behavior because they are overshadowed by the divergences at both interfaces. To overcome this inconvenience, we introduced finite renormalized quantities $\tilde{w}_i(z)$ (i = 1, 2, 3) by taking the product of the divergent $w_i(z)$ at the interfaces and the corresponding factor $f_i(z)$ from the set $\{f_i(z)\} = \left\{\left|z - \frac{1}{2}\right|^3, \left|z - \frac{1}{2}\right|^3 \left|z + \frac{1}{2}\right|^3, \left|z + \frac{1}{2}\right|^3\right\}$, i.e., $\tilde{w}_i(z) = w_i(z) f_i(z)$ with i = 1, 2, 3. Those factors eliminate the indicated divergence in $w_i(z)$ and provide an opportunity to obtain information on the short- and long-range asymptotic behavior of $w_i(z)$ in the layers [see Figs. 2(b)–4(b); note that the scale along the axis z within the interval $-\frac{1}{2} \le z \le \frac{1}{2}$ differs from that beyond it]. In particular, in the case of medium 1, the multiplier $f_1(z) = \left|z - \frac{1}{2}\right|^3$ makes it possible

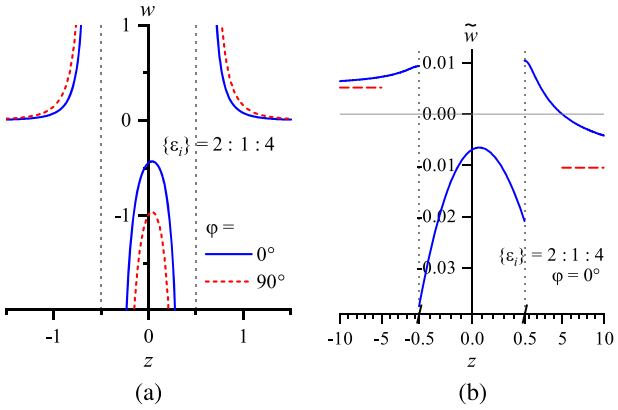

FIG. 2. (a) Dependence of the dimensionless image force energy $w = L^3 W^{pd}/P^2$ for a point dipole with the moment P on the dimensionless dipole coordinate $z = Z/L$ calculated in all three layers of a heterostructure with $\{\varepsilon_i\} = 2 : 1 : 4$. Solid and dashed curves correspond to the parallel ($\varphi = 0°$) and perpendicular ($\varphi = 90°$), respectively, dipole orientations relative to the interfaces. (b) Finite dependence $\tilde{w}(z)$ obtained by excluding divergent factors from $w(z)$. The angle $\varphi = 0°$. Dashed horizontal lines represent long-range asymptotic values in the covers. See explanations in the text.

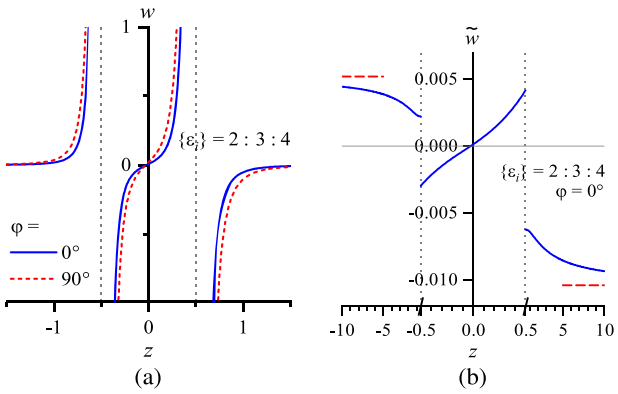

FIG. 3. [(a) and (b)] The same as in Fig. 2, but for $\{\varepsilon_i\} = 2 : 3 : 4$.

to simultaneously evaluate and compare the coefficients both in the most divergent term (16), at the $z = \frac{1}{2}$ interface, and in the long-range asymptotics (14). The absolute-value mode for the renormalizing factors was selected to preserve information about the w-sign (repulsion or attraction).

The renormalizing factor $f_2(z) = \left|z - \frac{1}{2}\right|^3 \left|z + \frac{1}{2}\right|^3$ selected for the interlayer also makes it possible to correctly evaluate the coefficient in the most divergent term at the proper interface. This is because one of its multiplier—in the case of $z = \frac{1}{2}$ interface, this is $\left|z - \frac{1}{2}\right|^3$—eliminates the divergence, whereas the other—this is $\left|z + \frac{1}{2}\right|^3$ in the case concerned—tends to unity and does not distort the value of the short-range asymptotic coefficient at this interface [see Eq. (17)]. The same is valid for the $z = -\frac{1}{2}$ interface as well. Then, we deduce that the $\tilde{w}$ values across the interfaces are related to each other as follows [see, e.g., Eqs. (16) and (17)]:

$$\frac{\tilde{w}_1\left(z = \frac{1}{2}\right)}{\tilde{w}_2\left(z = \frac{1}{2}\right)} = -\frac{\varepsilon_2}{\varepsilon_1}, \quad \frac{\tilde{w}_3\left(z = -\frac{1}{2}\right)}{\tilde{w}_2\left(z = -\frac{1}{2}\right)} = -\frac{\varepsilon_2}{\varepsilon_3}.$$

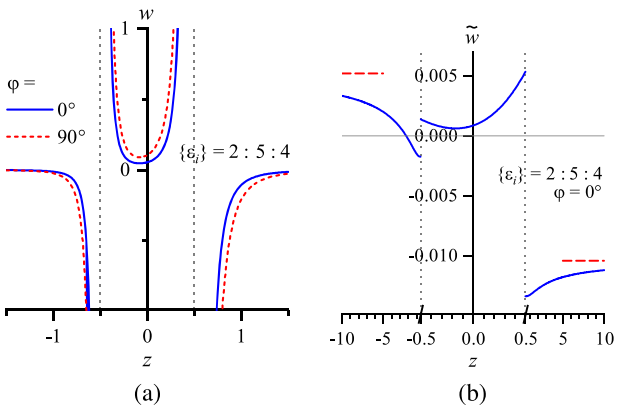

FIG. 4. [(a) and (b)] The same as in Fig. 2, but for $\{\varepsilon_i\} = 2 : 5 : 4$.

The values of the coefficients in the long-range asymptotics of $w(z)$ in the covers are also indicated in Figs. 2(b)–4(b) by dashed horizontal lines. Attention is attracted by the following fact (and it will be reproduced in other calculations given below): As the distance from the slab toward both sides increases, the $w(z)$ values diminish much more rapidly [$w(z) \sim z^{-3}$] than it would be in the case of a single point charge [$w(z) \sim z^{-1}$]. Nevertheless, it turned out that the corresponding long-range asymptotic limits are reached only at very large distances from the slab.

Below, in order to illustrate the properties of the obtained solution (11)–(13), we consider the influence of certain system parameters on $w(z)$ and its asymptotics in some most interesting, from our viewpoint, cases. However, we would like to attract attention that the general solution can be expressed as functions of the normalized coordinate $z = Z/L$. The latter can be varied by (i) moving the dipole normally to the heterostructure interfaces and leaving the interlayer width L intact or (ii) changing the slab width L and properly modifying the coordinate Z.

Now, let us consider a dipole in vacuum (medium 1, $\varepsilon_1 = 1$) over various substrates (medium 3, $\varepsilon_3 = \text{var}$) covered with a film (medium 2) with $\varepsilon_2 = 3$. From the rules given above, it follows that the slab always exerts an attractive action on the dipole ($\varepsilon_1 < \varepsilon_2$). The substrate always attracts the dipole (if $\varepsilon_2 > 1$ so that $\varepsilon_1 < \varepsilon_2$). If $\varepsilon_2 = 1$, so that $\varepsilon_1 = \varepsilon_2$, the substrate remains "indifferent" with respect to the dipole, but the slab provides the general attraction in this case as well. Thus, the dipole is always attracted to the substrate at any ε_3. The results of calculations for the dependence $w_1(z)$, which are exhibited in Fig. 5(a), confirm this rather trivial conclusion.

More information can be obtained when analyzing the corresponding renormalized $\tilde{w}_1(z)$ dependences [Fig. 5(b)]. According to Eq. (16), where the coefficient is ε_2-independent in the case concerned, the curves form a node at $z = \frac{1}{2}$. At the same time, they have different values at $z \to \infty$, which satisfy Eq. (14). We draw attention to the result obtained for $\varepsilon_3 = 3$, which is depicted by the horizontal dashed line [its counterpart in panel (a) is also shown by the dashed curve]. In this case, $\varepsilon_2 = \varepsilon_3 \neq \varepsilon_1$, and we obtain a two-layer system, in which $w_1(z)$ is described by formula (18), so that the short- and long-range asymptotic coefficients coincide. In other variants, with $\varepsilon_2 \neq \varepsilon_3$, this is not the case, and we can observe how slowly the curves in panel (b) approach their corresponding long-range ($z \to \infty$) asymptotics.

Now, let us put the dielectric constant of the substrate $\varepsilon_3 = 3$ and vary the dielectric constant ε_2 of the interlayer (Fig. 6). The system remains strictly "attractive," as in the previous case, and the qualitative behavior of the $w_1(z)$ dependences also remains the same [cf. Figs. 5(a) and 6(a)]. Furthermore, the curve for $\varepsilon_2 = 3$ in Fig. 6(a) is identical to the curve for $\varepsilon_3 = 3$ in Fig. 5(a) because they describe the same system with $\{\varepsilon_i\} = 1 : 3 : 3$. Subtle differences can be observed between the corresponding $\tilde{w}_1(z)$ dependences [cf. Figs. 5(b) and 6(b)]. Here, we have an inverse situation in comparison with the previous case. Specifically, at $z = \frac{1}{2}$, the curves acquire different values dictated by the same relationship (16) and they tend to the same value satisfying formula (14) at $z \to \infty$.

Almost the same situation (with an accuracy of the w_1- and $\tilde{w}_1$-sign change) will take place in the purely "repulsive" configuration, when $\varepsilon_1 > (\varepsilon_2, \varepsilon_3)$. Hence, it will not be illustrated at length.

The most interesting situations occur if the interlayer and the substrate have different (repulsive or attractive) influences on the

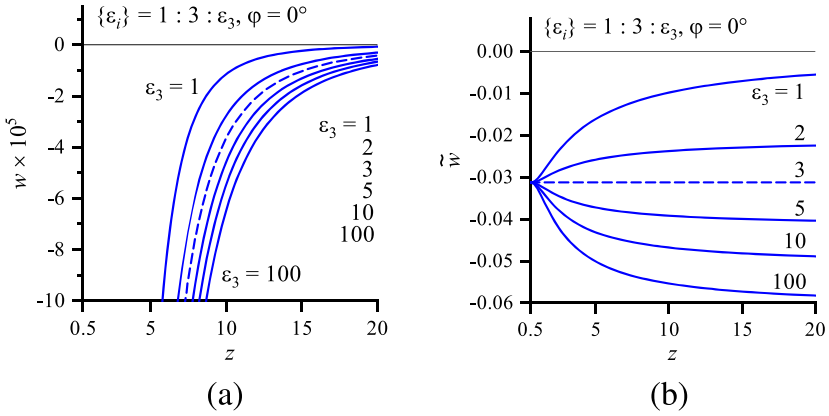

FIG. 5. Dependences (a) $w(z)$ and (b) $\widetilde{w}(z)$ in medium 1 for $\varphi = 0°$ and $\{\varepsilon_i\} = 1 : 3 : \varepsilon_3$. Dashed curves correspond to $\{\varepsilon_i\} = 1 : 3 : 3$, i.e., a two-layer system.

dipole. Let us first illustrate the case when the dielectric permittivity of the substrate (medium 3) is fixed, whereas that of the interlayer is varied (Fig. 7). Here, we have two possibilities: the substrate attracts the dipole located in medium 1 far from the interlayer [panel (a)] or repulses it [panel (b)]. In the former case ($\varepsilon_3 > \varepsilon_1$), by varying ε_2, we can select either the purely attractive mode for the dipole ($\varepsilon_2 > \varepsilon_1$) or the mode with the formation of a potential barrier ($\varepsilon_2 < \varepsilon_1$). Those modes are separated by a certain ε_2-value ($\varepsilon_2 = \varepsilon_1 = 3$ in the case concerned) at which the interlayer becomes "neutral" with respect to the medium where the dipole is located; nevertheless, the substrate provides the overall attraction in this case (the dashed curve).

An analogous situation is observed in the latter case with the repulsive substrate ($\varepsilon_3 < \varepsilon_1$). The pure repulsion of the dipole in the whole cover 1 can be guaranteed only if the interlayer also plays a repulsive ($\varepsilon_2 > \varepsilon_1$) or at least a "neutral" ($\varepsilon_2 = \varepsilon_1$) role. The scenarios with the fixed interlayer and varied substrate permittivities are illustrated in Fig. 8.

However, expression (11) for $w_1(z)$ also contains the φ-dependent factor $1 + \sin^2\varphi$ that varies from 1 at $\varphi = 0°$ to 2 at $\varphi = 90°$. It is easy to understand (see Fig. 9) that we have $w_1(z, \varphi = 0°) < w_1(z, \varphi = 90°)$ at those z's where w_1 is positive and $w_1(z, \varphi = 0°) > w_1(z, \varphi = 90°)$ in the intervals where w_1 is negative. It means that, at any z, the dipole acquires a preferential orientation that is energetically more advantageous: parallel ($\varphi = 0°$) if $w_1(z) > 0$ or perpendicular ($\varphi = \pm 90°$) if $w_1(z) < 0$ (thick curve in Fig. 9). From Figs. 7 and 8, the specific orientation (e.g., whether the dipole located near the interlayer is parallel or perpendicular to it) depends on the specific combination of ε_i values. We should emphasize that the preferential orientations of real molecules with permanent dipole moments depend on various other contributing factors and can differ from the indicated values.

In the conventional scenario, the short-range repulsion of the molecule at the interface is attributed to the quantum mechanical effects (frequently called the Pauli repulsion between the overlapping electron wave functions of the adsorbed molecule and the substrate).[10,13,20,29,75–82] This effect unavoidably exists for adsorbates located close to the surface. Nevertheless, the results demonstrated in Fig. 7(b) testify that the adsorption may be prevented electrostatically for quite reasonable values of thin-film dielectric permittivities. Purely electrostatic repulsion starts at the distances z of the molecules from the film that exceed the distances at which the Pauli repulsion emerges. Of course, when ε_2 grows and becomes large enough (in our case, it happens at $\varepsilon_2 \geq 10$), the influence of the substrate vanishes and the dipole is attracted to the film until the short-range Pauli repulsion (by no means treated in this classical

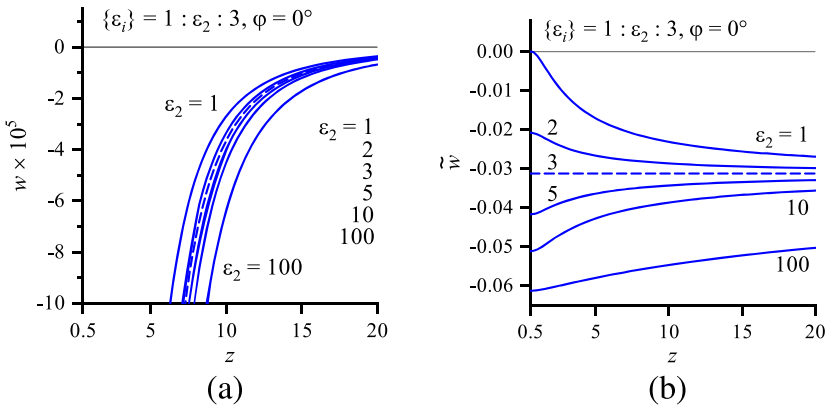

FIG. 6. [(a) and (b)] The same as in Fig. 5, but for $\varphi = 0°$ and $\{\varepsilon_i\} = 1 : \varepsilon_2 : 3$.

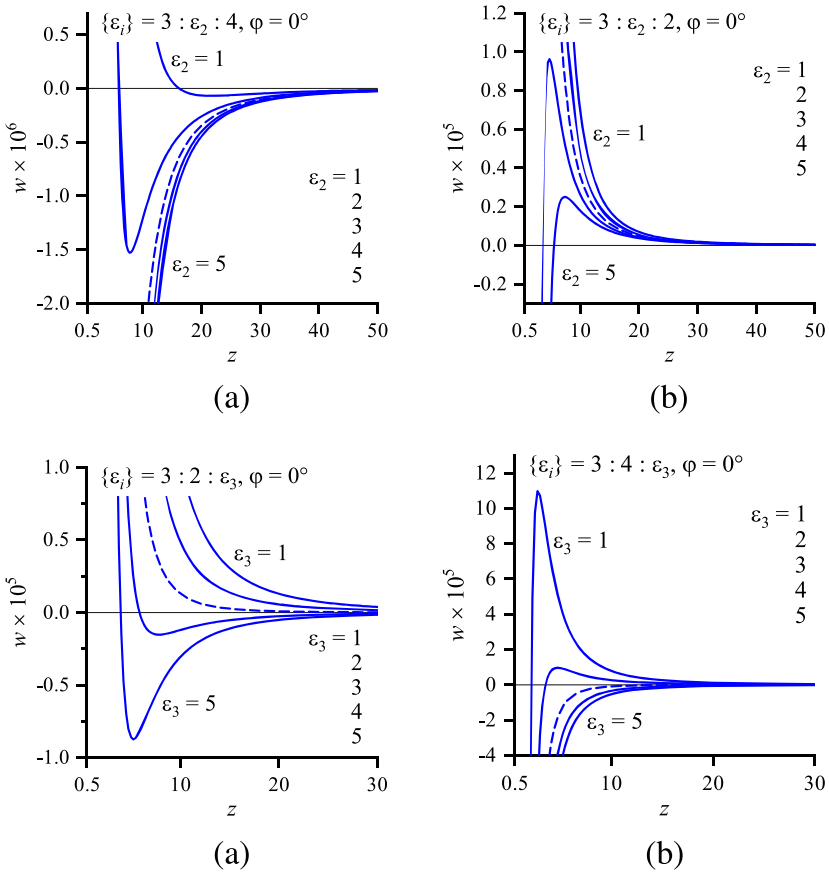

FIG. 7. Dependences $w(z)$ in medium 1 for $\varphi = 0°$ and (a) $\{\varepsilon_i\} = 3 : \varepsilon_2 : 4$ or (b) $\{\varepsilon_i\} = 3 : \varepsilon_2 : 2$. Dashed curves correspond to the equality $\varepsilon_2 = \varepsilon_1$ and separate the monotonic and non-monotonic $w(z)$ dependences.

FIG. 8. The same as in Fig. 7, but for (a) $\{\varepsilon_i\} = 3 : 2 : \varepsilon_3$ or (b) $\{\varepsilon_i\} = 3 : 4 : \varepsilon_3$. Dashed curves correspond to the equality $\varepsilon_3 = \varepsilon_1$.

approach!) stops it at a certain equilibrium distance. Thus, it turns out that a purely electrostatic mechanism controlling the molecular adsorption in three-layer sandwiches is possible. However, these conclusions should be checked by applying more sophisticated models of heterostructures in which the spatial dispersion of dielectric permittivity (permittivities) is made allowance for.[23,24]

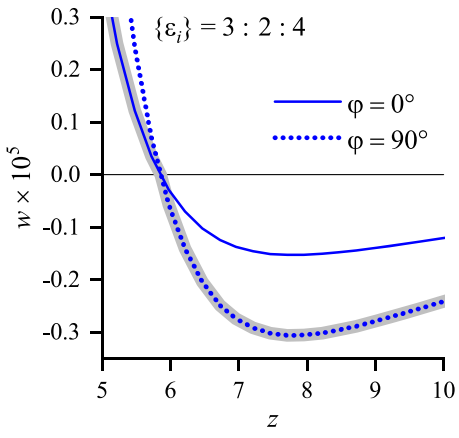

FIG. 9. Fragments of the $w(z)$ dependences for $\{\varepsilon_i\} = 3 : 2 : 4$ and various φ's.

On the other hand, a subtle interplay between purely classical electrostatic attraction of the dipole to and its repulsion from polarization charges arising at both interfaces may confine dipoles at the heterostructure interfaces, which means their physical adsorption. The confined dipoles in this scenario are located at large distances z's from the film as compared with its thickness L. The corresponding minimum in the dipole image force energy was found long ago.[50] However, those results are totally unreliable, since we have found that even the starting formulas are wrong. Hence, the final ones cannot be correct either. The possibility of electrostatic adsorption revealed in our calculations may be, in particular, important for large organic molecules,[34,73,80] which can be confined in wide wells of the type shown in Figs. 5(a) and 6(a).

The electrostatic well for point-like dipoles is analogous to the well arising for point charges near the interface between an insulator and a plasma-like medium[83] (see also Refs. 70 and 84). In the latter model, the inverse Thomas–Fermi (for the quantum plasma of a metal) or Debye–Hückel (for the classical plasma or electrolyte) length λ (see the analysis of possible cases in Ref. 85) plays a similar role as the slab width L does in our problem.

To finish the analysis of the dipole behavior in the cover, let us consider the $w_1(z)$ dependences in the symmetric case, i.e., for

a slab with varying ε_2 sandwiched between two identical electrodes with $\varepsilon_1 = \varepsilon_3$, which is met, in practice, rather frequently (see Fig. 10). In this case, the substrate is inert with respect to the dipole-induced image force, and it is only the dielectric permittivity ε_2 of the slab that governs the attraction or repulsion of the latter at all distances. The corresponding dependences are rigorously monotonic [except for the degenerate state $\varepsilon_1 = \varepsilon_2 = \varepsilon_3$, see Eq. (20)] and are characterized by the long-range z^{-4} asymptotics [Eq. (15)].

From Figs. 2–4, from the electrostatic viewpoint, the most energetically beneficial position of a dipole inside the slab crucially depends on the relationship between the medium dielectric constants. However, strictly speaking, electrostatically driven molecules can either concentrate near the $z = \pm\frac{1}{2}$ interfaces [if $w_2(z)$ has a maximum or an inflection point] or be adsorbed inside the slab far from its boundaries [if $w_2(z)$ has a minimum]. The latter case is the most interesting for applications, since in such a way molecules can be confined in the heterostructure interlayer. In Fig. 11, the renormalized dependences $\tilde{w}_2(z)$ are depicted for slabs with various ε_2's suspended in the vacuum or gas vapor. We note that the angular dependence of w_2, according to Eq. (12), is not reduced to the trivial factor $\left(1 + \sin^2\varphi\right)$ so that we had to demonstrate the ultimate cases of the dipole oriented perpendicularly or in parallel to the layer planes. Nevertheless, both sets of dependences turned out to be very similar.

Let us now compare our results with the previous attempts of the predecessors[50,73] dealing with the same problem. First of all, none of them managed to obtain the final correct formulas (11)–(13). The reason of their failure is quite clear: they did not start from the general approach[23,24,53,54,56] already elaborated for point charges but investigated various particular cases. Furthermore, no final explicit analytical dependences of the image force energy on z were obtained! Moreover, even the presented particular results turn out wrong. Indeed, as can be seen from (12), the dependence $w_2(z)$ includes two terms with the standard angular factor $\left(1 + \sin^2\varphi\right)$ and one z-independent (!) term with the angular factor $\left(1 - 3\sin^2\varphi\right)$ so that the total angular dependence of the point-dipole energy in the slab becomes anomalous. The absence of the nonstandard term clearly indicates that the calculations led to erroneous results. To summarize this comparison, we emphasize that the problem of the dipole image force energy in three-layer systems has been solved here for the first time and its validity is confirmed in all limiting cases.

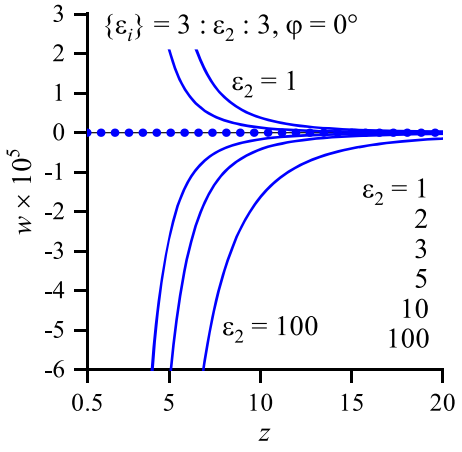

FIG. 10. The same as in Fig. 6(a), but for $\varphi = 0°$ and $\{\varepsilon_i\} = 3 : \varepsilon_2 : 3$.

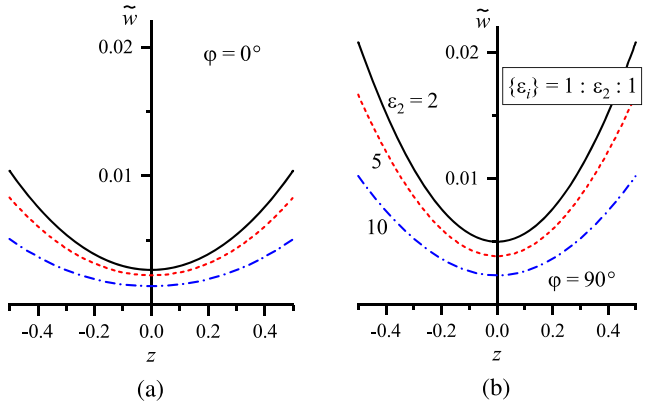

FIG. 11. Dependences $\tilde{w}(z)$ in medium 2 at $\{\varepsilon_i\} = 1 : \varepsilon_2 : 1$ and for (a) $\varphi = 0°$ and (b) $\varphi = 90°$.

To elucidate the role of the z-independent interference term in Eq. (12) (the interference constant), let us first make some analytical calculations for a peculiar point, namely, the slab center ($z = 0$), in a symmetrical sandwich with metal covers. In this case, $\varepsilon_1 = \varepsilon_3 \to \infty$ and a finite $\varepsilon_2 \geq 1$ so that $\theta = -1$. Then, in formula (12), we have $\Phi\left(1, \frac{1}{2}, 3\right) = 7\zeta(3)$ and $\Phi(1,1,3) = \zeta(3)$, where $\zeta(x)$ is the Riemann zeta function,[72] and the expression for w_2 takes a simple form

$$w_2(z = 0, \varepsilon_2 \geq 1, \varepsilon \to \infty) \to -\frac{\zeta(3)}{4\varepsilon_2}\left(3 + 5\sin^2\varphi\right). \tag{21}$$

This limiting case clearly demonstrates that the interference constant distorts the classical angular dependence.

The existence of z-independent term in expression $w_2(z)$ is unavoidable, but it only shifts the $w_2(z)$ profile as a whole along the ordinate axis and does not change the character of this dependence {with a maximum, a minimum, or an inflection point [see Figs. 2(a)–4(a)]}. Indeed, the terms in Eq. (12), singular at the corresponding interfaces, must compensate each other at some point (not necessarily at $z = 0$ if the heterostructure is non-symmetric). This is true not only for the dipole image force energies but also for their constituents, i.e., the image force energies for point charges. The latter statement can be understood if one examines the textbook expression for the charge polarization energy $W_{\rm ch}^{\rm met}(Z)$ in the vacuum gap between metal electrodes,[30]

$$W_{\rm ch}^{\rm met}(Z) = \frac{Q^2}{4L}\left[2\log\gamma + \psi\left(\frac{1}{2} - \frac{Z}{L}\right) + \psi\left(\frac{1}{2} + \frac{Z}{L}\right)\right],$$

where an interference constant

$$W_{\rm ch}^{\rm met}(Z = 0) = -\frac{Q^2\log 2}{L} \tag{22}$$

appears in the center of the gap. Here, $\gamma = 1.78\ldots$ is the Euler constant, and $\psi(x)$ is the logarithmic derivative of the gamma function.

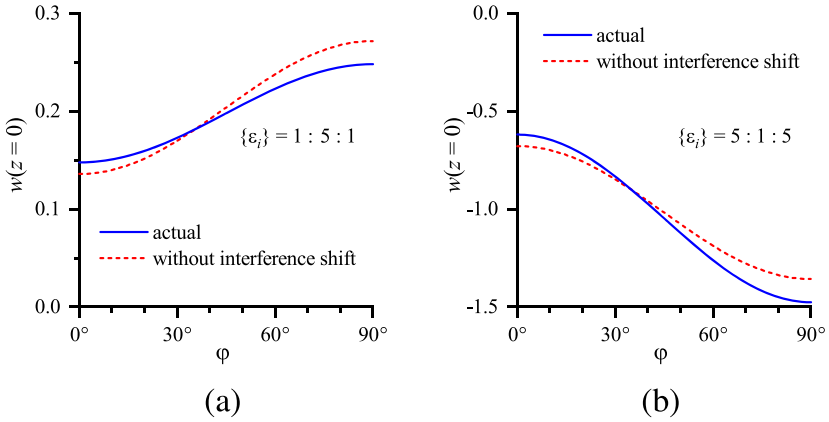

FIG. 12. Dependences of $w(z = 0)$ on φ in medium 2 for (a) $\{\varepsilon_i\} = 1 : 5 : 1$ and (b) $\{\varepsilon_i\} = 5 : 1 : 5$. The solid curve corresponds to the actual dependence. The dashed curve describes the dependence obtained without the account of the constant interference term (see explanations in the text).

Moreover, let us analyze the energy $W_{\rm ch}^{\rm ins}(Z)$ in the case of a symmetric sandwich with $\varepsilon_1 = \varepsilon_3 = \varepsilon \neq \varepsilon_2$. In this case, it was shown[56] that, with an accuracy of at least 6% (in reality, the numerical and approximate curves coincide graphically), this quantity can be represented as the sum of the combined image force energies at both the interfaces and the interference term

$$W_{\rm ch}^{\rm ins}(Z) = -\frac{Q^2}{\varepsilon_2 L}\left[\log\left(\frac{2\varepsilon}{\varepsilon+\varepsilon_2}\right) + \frac{4(\varepsilon-\varepsilon_2)Z^2}{(\varepsilon+\varepsilon_2)(L^2-4Z^2)}\right]. \qquad (23)$$

Thus, the Z-independent interference constant constitutes an additional term to the conventional polarization energies at the interfaces. The same is true for dipoles, as comes about from Eq. (12). On the contrary, popular Simmons approximation formulas[86,87] for point-charge image forces in the inter-electrode gap are wrong from the theoretical point of view because the interference constant is not isolated in Refs. 86 and 87 and is treated as a factor distorting the superposition of both image-force contributions.

The angular dependences of $w_2(z = 0)$ characterizing simple symmetric sandwiches are displayed in Fig. 12 for the cases of the maximum [panel (a)] and minimum [panel (b)] in the slab center. Solid curves correspond to the actual (full) dependences, whereas the interference constant was subtracted from $w_2(z = 0)$ for their dashed counterparts. It is clear from the comparison of the solid and dashed curves that a peculiar angular dependence $\left(1 - 3\sin^2\varphi\right)$ of the interference term does not alter the overall tendency dictated by the "normal" dependence $\left(1 + \sin^2\varphi\right)$. For instance, in the case of resulting attraction [Fig. 12(b)], the latter is stronger at the maximum point for perpendicularly oriented dipoles, no matter whether the interference constant is made allowance for or not.

The results of our calculations showed that, if the dipole in the interlayer has the same interaction type (attraction or repulsion) with both covers, the corresponding $w_2(z)$ dependence preserves its sign across the interlayer [see Figs. 2(a) and 4(a)]. Therefore, taking the aforesaid into account and examining Figs. 2(a)–4(a) on the basis of the same arguments that were used when discussing Fig. 9, a conclusion can be drawn that the dipole can change its preferential orientation across the slab only in the "monotonic" cases $\varepsilon_1 < \varepsilon_2 < \varepsilon_3$ and $\varepsilon_1 > \varepsilon_2 > \varepsilon_3$.

V. CONCLUSIONS

In this article, we showed that the image force energy for permanent point dipoles in three-layer structures, $W^{\rm pd}(Z)$, can be calculated exactly in the framework of classical electrostatics. The resulting formulas clearly demonstrate that $W^{\rm pd}$ includes contributions from polarization charges at both interfaces involved. When being in any cover close to the slab, a dipole feels mainly the latter influence. At the same time, when it is far away from the slab, this limit corresponds to the infinitesimally thin interlayer. As a result, the dipole is influenced by the polarization charges at both interfaces on an equal footing, and the slab parameters fall out of the final expression.

The difference between the dielectric constants of the layers may lead to two interesting phenomena, which can be observed for dipoles located in the covers. First, the electrostatic repulsion induced by a thin film can prevent adsorption of polar molecules. Second, the electrostatic well can appear far away from the film surface. A molecule may be trapped in this well without any involvement of the quantum mechanical Pauli repulsion of the molecule's electron shells from those of the slab atoms (molecules). One might also speculate that the unconventional purely electrostatic control of the dipole location in heterostructures has some relation to the unexpected bright photoluminescence in carbon nanodots.[88]

If the dipole is located inside the slab, for instance, in a gap between two electrodes, it interacts with both of them so that the results are very peculiar, namely, the interference constant appears having the dependence on the dipole orientation angle φ different from those of the other terms, which are the textbook ones $\left(1 + \sin^2\varphi\right)$.

The new formulas obtained are interesting *per se*, but they can also be used in the physics and chemistry of adsorption[1,3–17] as the input functions. We note that the adopted method[53,54,58,59] makes it possible to calculate $W_{ii}^{\rm pd}$ in a more general case, when the spatial dispersion of the dielectric permittivities for all media is taken into consideration. In particular, by doing so, we can get rid of the divergences at the interfaces intrinsic to the classical approach, as has already been done for dipole image forces in the two-layer structures.[18,23,24] Nevertheless, the whole structure of the final formulas will remain the same so that the conclusions made here will survive

in a more complicated analysis. At the same time, the classical electrostatic calculations are transparent and give a useful insight into the problem.

ACKNOWLEDGMENTS

This work was partially supported by Project No. 22 of the 2018–2020 Scientific Cooperation Agreement between Poland and Ukraine, the NAS of Ukraine (Grant Nos. 1.4.B-179 and VC-205), and the Polish Academy of Sciences (NCN Grant No. 2015/19/B/ST4/02721).

REFERENCES

[1] A. A. Kornyshev and M. A. Vorotyntsev, Surf. Sci. **101**, 23 (1980).
[2] M. K. Gilson, A. Rashin, R. Fine, and B. Honig, J. Mol. Biol. **184**, 503 (1985).
[3] W. Schmickler and D. Henderson, Prog. Surf. Sci. **22**, 323 (1986).
[4] W. Mönch, Rep. Prog. Phys. **53**, 221 (1990).
[5] *Electrified Interfaces in Physics, Chemistry and Biology*, edited by R. Guidelli (Springer-Verlag, Dordrecht, 1992).
[6] W. R. Fawcett, *Liquids Solutions, and Interfaces: From Classical Macroscopic Descriptions to Modern Microscopic Details* (Oxford University Press, Oxford, 2004).
[7] A. M. Gabovich, Yu. A. Reznikov, and A. I. Voitenko, Phys. Rev. E **73**, 021606 (2006).
[8] Z. Adamczyk, *Particles at Interfaces: Interactions, Deposition, Structure* (Academic Press, Amsterdam, 2006).
[9] G. Barbero and L. R. Evangelista, *Adsorption Phenomena and Anchoring Energy in Nematic Liquid Crystals* (Taylor & Francis Ltd., Boca Raton, FL, 2006).
[10] H. Y. Erbil, *Surface Chemistry of Solid and Liquid Interfaces* (Blackwell Publishing, Oxford, 2006).
[11] A. A. Kornyshev, D. J. Lee, S. Leikin, and A. Wynveen, Rev. Mod. Phys. **79**, 943 (2007).
[12] *Surface and Interface Science*, Concepts and Methods Vol. 1, edited by K. Wandelt (Wiley-VCH Verlag, Weinheim, 2012).
[13] *Surface and Interface Science*, Properties of Elemental Surfaces Vol. 2, edited by K. Wandelt (Wiley-VCH Verlag, Weinheim, 2012).
[14] *Surface and Interface Science*, Properties of Composite Surfaces: Alloys, Compounds, Semiconductors Vol. 3, edited by K. Wandelt (Wiley-VCH Verlag, Weinheim, 2014).
[15] *Surface and Interface Science*, Solid-Solid Interfaces and Thin Films Vol. 4, edited by K. Wandelt (Wiley-VCH Verlag, Weinheim, 2014).
[16] M. V. Fedorov and A. A. Kornyshev, Chem. Rev. **114**, 2978 (2014).
[17] D. P. Woodruff, Jpn. J. Appl. Phys. **58**, 100501 (2019).
[18] P. R. Antoniewicz, J. Chem. Phys. **56**, 1711 (1972).
[19] P. R. Antoniewicz, Surf. Sci. **52**, 703 (1975).
[20] S. Holmström and S. Holloway, Surf. Sci. **173**, L647 (1986).
[21] *Current Topics in Membranes and Transport*, edited by F. Bronner and A. Kleinzeller (Academic Press, New York, 1977), Vol. 9.
[22] A. Kokalj, Electrochim. Acta **56**, 745 (2010).
[23] A. M. Gabovich, M. S. Li, H. Szymczak, and A. I. Voitenko, Surf. Sci. **606**, 510 (2012).
[24] A. M. Gabovich, V. M. Gun'ko, V. E. Klymenko, and A. I. Voitenko, Eur. Phys. J. B **85**, 284 (2012).
[25] J. Fraxedas, *Water at Interfaces. A Molecular Approach* (CRC Press, Boca Raton, 2014).
[26] A. Kokalj, Phys. Rev. B **84**, 045418 (2011).
[27] A. M. Gabovich and A. I. Voitenko, Low Temp. Phys. **42**, 661 (2016).
[28] A. M. Gabovich and A. I. Voitenko, J. Mol. Liq. **267**, 166 (2018).
[29] H.-J. Butt and M. Kappl, *Surface and Interfacial Forces* (Wiley-VCH Verlag, Weinheim, 2018).
[30] W. R. Smythe, *Static and Dynamic Electricity* (McGraw-Hill, New York, 1950).
[31] S. F. Mahmoud, IEEE Trans. Antennas Propag. **32**, 679 (1984).
[32] O. Manasreh, *Semiconductor Heterojunctions and Nanostructures* (McGraw-Hill, New York, 2005).
[33] J. C. W. Song and N. M. Gabor, Nat. Nanotechnol. **13**, 986 (2018).
[34] D. Schuhmann, J. Electroanal. Chem. **201**, 247 (1986).
[35] F. Bechstedt and M. Scheffler, Surf. Sci. Rep. **18**, 145 (1993).
[36] H. Bluhm, T. Inoue, and M. Salmeron, Surf. Sci. **462**, L599 (2000).
[37] *The Molecule-Metal Interface*, edited by N. Koch, N. Ueno, and A. T. S. Wee (Wiley-VCH Verlag, Weinheim, 2013).
[38] *Landolt-Börnstein: Numerical Data and Functional Relationships in Science and Technology. New Series: Group III: Condensed Matter*, Physics of Solid Surfaces Vol. 45, Subvolume A, edited by G. Chiarotti and P. Chiaradia (Springer-Verlag, Berlin, 2015).
[39] J. Kerfoot, V. V. Korolkov, A. S. Nizovtsev, R. Jones, T. Taniguchi, K. Watanabe, I. Lesanovsky, B. Olmos, N. A. Besley, E. Besley, and P. H. Beton, J. Chem. Phys. **149**, 054701 (2018).
[40] F. Hidalgo, A. Rubio-Ponce, and C. Noguez, J. Phys. Chem. C **123**, 15273 (2019).
[41] S. McLaughlin, in *Current Topics in Membranes and Transport*, edited by F. Bronner and A. Kleinzeller (Academic Press, New York, 1977), Vol. 9, p. 71.
[42] H. Möhwald, Annu. Rev. Phys. Chem. **41**, 441 (1990).
[43] E. von Kitzing and D. M. Soumpasis, Biophys. J. **71**, 795 (1996).
[44] R. R. Netz, Eur. Phys. J. E **3**, 131 (2000).
[45] T. Ambjörnsson, M. A. Lomholt, and P. L. Hansen, Phys. Rev. E **75**, 051916 (2007).
[46] H. Lin, Z. Xu, H. Tang, and W. Cai, J. Sci. Comput. **53**, 249 (2012).
[47] K. Cahill, Phys. Rev. E **85**, 051921 (2012).
[48] S. Buyukdagli, J. Phys.: Condens. Matter **27**, 455101 (2015).
[49] S. Buyukdagli and R. Podgornik, Phys. Rev. E **99**, 062501 (2019).
[50] J. P. Badiali and M. L. Rosinberg, J. Electroanal. Chem. **122**, 45 (1981).
[51] Yu. A. Romanov, Zh. Éksp. Teor. Fiz. **47**, 2119 (1964).
[52] A. M. Gabovich, L. G. Il'chenko, E. A. Pashitskii, and Yu. A. Romanov, Zh. Éksp. Teor. Fiz. **75**, 249 (1978).
[53] A. M. Gabovich, L. G. Il'chenko, E. A. Pashitskii, and Yu. A. Romanov, Surf. Sci. **94**, 179 (1980).
[54] L. G. Il'chenko, E. A. Pashitskii, and Yu. A. Romanov, Surf. Sci. **121**, 375 (1982).
[55] F. Bechstedt and R. Enderlein, Phys. Status Solidi B **131**, 53 (1985).
[56] A. M. Gabovich, V. M. Rosenbaum, and A. I. Voitenko, Surf. Sci. **186**, 523 (1987).
[57] E. P. Pokatilov, V. M. Fomin, and S. I. Beril, *Oscillatory Excitations, Polarons and Excitons in Multilayer Systems and Superlattices* (Shtiintsa, Kishinev, 1990) (in Russian).
[58] A. M. Gabovich and A. I. Voitenko, Condens. Matter **4**, 44 (2019).
[59] A. M. Gabovich, M. S. Li, H. Szymczak, and A. I. Voitenko, J. Electrostat. **102**, 103377 (2019).
[60] J. W. Gadzuk, Solid State Commun. **5**, 743 (1967).
[61] D. M. Newns, J. Chem. Phys. **50**, 4572 (1969).
[62] D. M. Newns, Phys. Rev. B **1**, 3304 (1970).
[63] J. W. Gadzuk, Surf. Sci. **23**, 58 (1970).
[64] A. V. Sidyakin, Zh. Éksp. Teor. Fiz. **58**, 573 (1970).
[65] J. Heinrichs, Phys. Rev. B **8**, 1346 (1973).
[66] A. A. Kornyshev, A. I. Rubinshtein, and M. A. Vorotyntsev, J. Phys. C: Solid State Phys. **11**, 3307 (1978).
[67] A. M. Gabovich and A. I. Voitenko, Electrochim. Acta **28**, 1771 (1983).
[68] H. Lichte and M. Lehmann, Rep. Prog. Phys. **71**, 016102 (2008).
[69] H. S. Harned and B. B. Owen, *The Physical Chemistry of Electrolytic Solutions* (Reinhold, New York, 1939).
[70] B. B. Smith and C. A. Koval, J. Electroanal. Chem. **277**, 43 (1990).
[71] Y. Levin, A. P. dos Santos, and A. Diehl, Phys. Rev. Lett. **103**, 257802 (2009).
[72] *Table of Integrals, Series and Products*, edited by I. S. Gradshteyn and I. M. Ryzhik (Academic Press, San Diego, CA, 2000).
[73] D. Schuhmann, J. Electroanal. Chem. **239**, 447 (1988).

[74]D. Schuhmann, J. Colloid Interface Sci. **134**, 152 (1990).
[75]*Interaction of Atoms and Molecules with Solid Surfaces*, edited by V. Bortolani, N. H. March, and M. P. Tosi (Springer-Verlag, New York, 1990).
[76]*Kelvin Probe Force Microscopy: From Single Charge Detection to Device Characterization*, edited by S. Sadewasser and T. Glatzel (Springer-Verlag, Cham, 2018).
[77]G. P. Brivio and M. I. Trioni, Rev. Mod. Phys. **71**, 231 (1999).
[78]C. Weiss, C. Wagner, C. Kleimann, M. Rohlfing, F. S. Tautz, and R. Temirov, Phys. Rev. Lett. **105**, 086103 (2010).
[79]K. Berland, V. R. Cooper, K. Lee, E. Schröder, T. Thonhauser, P. Hyldgaard, and B. I. Lundqvist, Rep. Prog. Phys. **78**, 066501 (2015).
[80]R. Hoffmann-Vogel, Rep. Prog. Phys. **81**, 016501 (2018).
[81]N. Moll, L. Gross, F. Mohn, A. Curioni, and G. Meyer, New J. Phys. **12**, 125020 (2010).
[82]N. Moll, L. Gross, F. Mohn, A. Curioni, and G. Meyer, New J. Phys. **14**, 083023 (2012).
[83]A. A. Kornyshev, A. I. Rubinshtein, and M. A. Vorotyntsev, Phys. Status Solidi B **84**, 125 (1977).
[84]B. E. Conway, Prog. Surf. Sci. **16**, 1 (1984).
[85]*The Dielectric Function of Condensed Systems*, edited by L. V. Keldysh, D. A. Kirzhnitz, and A. A. Maradudin (North-Holland, Amsterdam, 1989).
[86]J. G. Simmons, J. Appl. Phys. **34**, 1793 (1963).
[87]J. G. Simmons, J. Appl. Phys. **34**, 2581 (1963).
[88]A. P. Demchenko, J. Carbon Res. **5**, 71 (2019).